Available online at www.sciencedirect.com
ScienceDirect
European Journal of Pharmacology 559 (2007) 21–31
www.elsevier.com/locate/ejphar

Differential effects of Ca^{2+} on bisphosphonate-induced growth inhibition in breast cancer and mesothelioma cells

Melinda A. Merrell [a,1], Savita Wakchoure [a,1], Joanna M. Ilvesaro [a], Kurt Zinn [a,b], Bradley Gehrs [a], Petri P. Lehenkari [c], Kevin W. Harris [a,d], Katri S. Selander [a,*]

[a] *Department of Medicine, Division of Hematology–Oncology, University of Alabama at Birmingham, WTI T558, 1824 6th Avenue South, Birmingham, AL 35294-3300, USA*
[b] *Laboratory for Multimodality Imaging, University of Alabama at Birmingham, Birmingham, AL, USA*
[c] *Clinical Research Centre, Department of Surgery, University of Oulu, Finland*
[d] *Birmingham Veterans Affairs Medical Center, Birmingham, AL, USA*

Received 1 August 2006; received in revised form 27 November 2006; accepted 29 November 2006
Available online 9 December 2006

Abstract

Bisphosphonates are widely clinically used inhibitors of bone resorption. Pre-clinical studies indicate that bisphosphonates also inhibit the growth of various cancer cells *in vitro*, but their *in vivo* anti-cancer activity varies greatly, depending on the tumor type. We compared the various cellular effects of bisphosphonates in breast cancer and mesothelioma cells, with differences in growth inhibition responses to bisphosphonate-treatment *in vivo*. We show that the growth inhibitory effects of nitrogen-containing bisphosphonates are significantly affected by excess Ca^{2+} in a cell- and bisphosphonate-specific fashion. Furthermore, excess pyrophosphate-resembling bisphosphonates prevent nitrogen-containing–bisphosphonate-induced accumulation of unprenylated Rap1A, p38 phosphorylation and growth inhibition in human MDA-MB-231 breast cancer and mouse AB-12 mesothelioma cells. For some, but not all tested, pyrophosphate-resembling bisphosphonate: nitrogen-containing bisphosphonate combinations these results may be partially explained by the ability of the excess pyrophosphate-resembling bisphosphonates to chelate Ca^{2+}. In mice, subcutaneous AB-12 and MDA-MB-231 tumors exhibit positive staining for Ca^{2+} minerals, as revealed with Von Kossa stainings. We further show that the AB-12 tumors accumulate significantly more of the bone scanning bisphosphonate, Tc99m-medronate, as compared with MDA-MB-231 tumors. In conclusion, our results suggest that Ca^{2+} regulates the growth inhibitory effects of bisphosphonates in a target cell and drug-specific fashion. These findings may be of physiological relevance since many tumor types are calcified. They further suggest that bisphosphonates can accumulate in tumors that are growing at the visceral sites and that differences in tumor accumulation of bisphosphonates may regulate their *in vivo* sensitivity to these drugs.

Keywords: Bisphosphonate; Breast cancer; Prenylation; p38; Mesothelioma

1. Introduction

Bisphosphonates are synthetic analogs of the naturally occurring pyrophosphate (Coxon et al., 2000; Rogers, 2004). They inhibit osteoclasts and are therefore widely clinically used in the treatment of disease conditions that are due to increased bone resorption, such as osteoporosis, solid tumor bone metastases and myeloma bone disease (Rodan and Martin, 2000).

Depending on their molecular structure, bisphosphonates can be divided into nitrogen-containing and pyrophosphate-resembling bisphosphonates, with different molecular mechanisms of action (Hosfield et al., 2004). Nitrogen-containing bisphosphonates, such as pamidronate, alendronate, risedronate and zoledronate inhibit the farnesyl pyrophosphate synthase in the mevalonate pathway, which results in decreased accumulation of prenyl groups inside the cells (van Beek et al., 1999). The lack of prenyl groups, such as geranylgeranyl, results in decreased post-translational prenylation of small GTP-binding proteins and thereby, impaired cellular functions, such as intracellular vesicular transportation in osteoclasts (Alakangas et al.,

* Corresponding author. Tel.: +1 205 975 5973; fax: +1 205 934 9511.
E-mail address: Katri.Selander@ccc.uab.edu (K.S. Selander).
[1] Equal contribution.

0014-2999/$ - see front matter © 2006 Elsevier B.V. All rights reserved.
doi:10.1016/j.ejphar.2006.11.064

2002; Rogers, 2004). Pyrophosphate-resembling bisphosphonates, such as clodronate and etidronate, do not inhibit the mevalonate pathway. Instead, they are metabolized in cells into ATP-like analogs, which mediate their cellular effects, such as apoptosis in osteoclasts (Lehenkari et al., 2002). Interestingly, however, it was shown recently that although nitrogen-containing bisphosphonates are not metabolized, they can still induce the formation of an endogenous, novel ATP analog (ApppI) in cells (Mönkkönen et al., 2006). Similar to the effects of the pyrophosphate-resembling bisphosphonate metabolite, ApppI also inhibits ADP/ATP translocase in isolated mitochondria and induces apoptosis in osteoclasts (Mönkkönen et al., 2006).

In addition to the effects on bone cells, the nitrogen-containing bisphosphonates especially have been shown to inhibit the growth of various cancer cells *in vitro* (Chuah et al., 2005; Iguchi et al., 2003; Merrell et al., 2003; Riebeling et al., 2002; Senaratne and Colston, 2002). This inhibition is probably at least partially mediated via inhibition of the mevalonate pathway, since in many cells it can be overcome by excess geranylgeraniol. Nevertheless, additional mechanisms may also exist (Reinholz et al., 2002). The *in vivo* anti-cancer efficacy of bisphosphonates varies greatly. While the efficacy of bisphosphonates in various breast cancer models has been shown to be marginal (Hiraga et al., 2001, 2004; Sasaki et al., 1995), especially the newer nitrogen-containing bisphosphonates have been shown to exhibit very strong anti-tumor activities in mouse models of metastatic osteosarcoma, mesothelioma, small cell lung and ovarian cancers (Hashimoto et al., 2005; Matsumoto et al., 2005; Ory et al., 2005; Sawada et al., 2002; Wakchoure et al., 2006). The reasons for these efficacy differences in the different cancer models are not understood. Furthermore, it is not even known whether the clinically used doses of bisphosphonates gain access into cancer cells (Powles et al., 2006, 2002; Saarto et al., 2001). Bisphosphonates are quickly, within minutes, cleared from the circulation and adsorbed to bone hydroxyapatite where they are retained (Skerjanec et al., 2003). Accumulation of the bone scanning agent, Tc99m-medronate, which is structurally a bisphosphonate, into tumors at the visceral site does, however, suggest that bisphosphonates may also gain access into tumors outside bones (Barai et al., 2004; Beres et al., 1991; Fogelman et al., 1978; Swayne et al., 1992; Tanabe et al., 1979; Vorne and Saukko, 1984). The mechanisms for this accumulation are not known.

It was shown recently that in osteoclasts and macrophages, excess pyrophosphate-resembling bisphosphonates can antagonize the cellular effects of nitrogen-containing bisphosphonates. This is possibly due to Ca^{2+}-chelation by the pyrophosphate-resembling bisphosphonates and thereby decreased Ca^{2+} availability for the nitrogen-containing bisphosphonates, resulting in their decreased cellular uptake (Frith and Rogers, 2003; Thompson et al., 2006a). Also the gamma delta T-cell receptor (γδTCR) and connexin-43 hemichannel have been shown to mediate bisphosphonate effects in various cells (Plotkin et al., 2005, 2002; Plotkin and Bellido, 2001; Sato et al., 2005; Thompson et al., 2006b). The aim of this study was to investigate whether similar mechanisms can be detected in breast cancer and mesothelioma cells. Furthermore, because of their different sensitivities to the anti-cancer effects of bisphosphonates *in vivo*, we investigated whether there are differences in tumor accumulation of Tc99m-medronate between breast cancer and mesothelioma cells *in vivo*.

2. Materials and methods

2.1. Chemicals

Bisphosphonates (risedronate, alendronate), were kindly provided by Leiras, Turku, Finland. Pamidronate (Pamidronate Disodium, Oncology Therapeutics Network, South San Fransisco, CA), zoledronate (Zometa, Novartis) and clodronate (Bonefos, Schering) were obtained from pharmacy. Stock solutions (10^{-2} or 10^{-3} M) were prepared into PBS, pH was adjusted to 7.4 with NaOH and filter-sterilized. Lipopolysaccharide (LPS) was from Sigma (St. Louis, MO), interleukin-1β (IL-1β) and tumor necrosis factor-α (TNF-α) were from R and D Systems (Minneapolis, MN). Geranylgeraniol (cold, all-*trans*) was from American Radiochemicals Inc. (St. Louis, MO), and prepared as a 100 mM stock solution in ethanol. Anti-Rap1A antibodies (SC-1482 and SC-65 for the detection of unprenylated Rap1A and total Rap1, respectively) were obtained from Santa Cruz Technology (San Diego, CA), anti-phospho p38 and total p38 antibodies were from Cell Signaling (Beverly, MA). Connexin-43 antibody was purchased from Zymed (San Fransisco, CA), the FITC-conjugated secondary antibody was from Chemicon (Melbourne, Australia). Lucifer yellow was purchased from Sigma and heptanol (prepared as a 3 M stock solution in ethanol) was from Fluka (Buchs, Switzerland), Tc99m-medronate (MDP-Bracco™) was bought from pharmacy.

2.2. Cell culture

Human MDA-MB-231 breast cancer and mouse AB-12 mesothelioma cells were maintained in Dulbecco's modified Eagle's medium (Life Technologies, Inc.) supplemented with 10% fetal calf serum (HyClone Laboratories, Logan, UT), 1% penicillin/streptomycin and non-essential amino acids (GIBCO BRL, Gaithersburg, ML). All cell cultures were done in incubators in a 37 °C atmosphere of 5% CO_2/95% air.

2.3. Western blot analysis

Cells were cultured on 6-well plates in normal culture medium until near confluency. The cells were then rinsed with sterile PBS and cultured for further 24 h in serum-free culture medium, in the presence or absence of the indicated bisphosphonates. Some cultures were also treated with 25 μM geranylgeraniol, 10 μg/ml LPS, 10 ng/ml IL-1β or TNF-α. To study bisphosphonate effects on connexin-43 expression, the cells were cultured for 24 h in serum-free culture medium in the presence of the indicated bisphosphonates or PBS as a vehicle control. Culture medium was then discarded, the cells were quickly lysed and prepared into Western blot samples, as

previously described in detail (Merrell et al., 2003). After boiling the supernatants in reducing sodium docedyl sulfate (SDS) sample buffer, equal amounts of protein (~20–50 μg) were loaded per lane and the samples were electrophoresed on 10% SDS polyacrylamide gel and transferred to a nitrocellulose membrane. To detect unprenylated Rap1A, the blots were incubated overnight at 4 °C with the antibody SC-1482, diluted 1:1000 in Tris-buffered saline, 0.1% (v/v) Tween-20 (TBST), and then with peroxidase-conjugated anti-goat serum (Pierce, Rockford, IL), diluted 1:1000 in TBST. Total Rap1 was detected from stripped blots in a similar fashion, with the antibody SC-65. The phosphorylation status of p38 was investigated using anti-phospho-p38 and after stripping of the membrane, with anti-total p38 antibodies, according to the manufacturer's instructions, as described before (Merrell et al., 2003). Expression of connexin-43 was detected with a rabbit anti-connexin-43 antibody (Zymed), diluted 1:1000 in TBST. The protein bands were visualized by chemiluminescence using SuperSignal West Pico ECL kit (Pierce, Rockford, IL).

2.4. Cell viability assays

Cells were plated on 96-well plates at the density of 1×10^3 cells in 100 μl per well in normal culture medium, with or without of the indicated concentrations of the various bisphosphonate combinations and/or 1 mM $CaCl_2$, 1 mM EGTA or vehicle and cultured for 48 h. Cell viability was assessed with 3-(4,5-dimethylthiazol-2-yl)-5-(3-carboxymethoxyphenyl)-2-(4-sulfophenyl)-2H-tetrazolium, inner salt (MTS)-assays (CellTiter Aqueous One 96, Promega, Madison, WI) according to the manufacturer's instructions. For each treatment, a PBS-control group was run simultaneously on the same plate. The results for each treatment were calculated as % of the corresponding PBS-group.

2.5. Connexin-43 immunofluorescence staining

MDA-MB-231 cells were fixed with 3% paraformaldehyde in PBS, permeabilized with 1% TritonX-100 in PBS, blocked with 2% bovine serum albumin (BSA)-PBS, and then stained with the anti-connexin-43 antibody (diluted 1:50 in 2% BSA-PBS) and with the appropriate secondary antibody. The stainings were visualized using a Zeiss fluorescent microscope (Thornwood, NY). Omission of the primary antibody served as a negative control for the staining.

2.6. Lucifer yellow uptake

Nitrogen-containing bisphosphonates have been shown to induce anti-apoptotic signals in osteocytes and osteoblasts specifically via the connexin-43 (Plotkin and Bellido, 2001; Plotkin et al., 2002). To investigate the possibility that bisphosphonate-induced hemichannel opening mediates the effects of these drugs also in breast cancer cells, Lucifer yellow uptake was studied in MDA-MB-231 cells here. To avoid cell to cell dye transfer, the cells were seeded at the density of 30 000 cells/well, which resulted in a sparse distribution of the cells. The cells were first incubated in serum-free conditions with ethanol or heptanol, a known inhibitor of gap junctions and hemichannels (Plotkin and Bellido, 2001), for 15 min. After this, the treatments (vehicle, 5 mM EGTA, 10^{-6} M alendronate or zoledronate) were added for further 15 min. Lucifer yellow (10 μg/ml) was added for the final 1 min after which the cells were washed with serum-free media to close the hemichannels again and fixed with 3% PFA-PBS. The cells were then stained with Hoechst (Sigma, 1 mg/ml stock prepared in ethanol and used in 1:800 dilution in PBS) to visualize nuclei, as previously described (Selander et al., 1996). Samples were viewed with fluorescent microscope to examine the uptake of Lucifer yellow (Plotkin and Bellido, 2001).

2.7. Flow cytometric analysis for γδTCR

MDA-231 cells were stained with a phycoerythrin-conjugated anti-γδ T-cell receptor (anti-γδ TCR) monoclonal antibody (clone 11F2; Becton Dickinson Biosciences, San Jose, CA). A phycoerythrin-conjugated, isotype matched irrelevant antibody served as a negative control. Cultured human blood mononuclear cells were used to exhibit positive staining. Analyses were performed using a FACSCalibur Flow cytometer (Becton Dickinson Biosciences, San Jose, CA) 7-aminoactinomycin D (Molecular Probes, Eugene, OR) was used to exclude nonviable cells. Data analysis was performed using CellQuest software (Becton Dickinson).

2.8. Tumor uptake of Tc99m-medronate

To investigate accumulation of the bone scanning agent (Tc99m-medronate) into the subcutaneous tumors, nude mice were first inoculated subcutaneously with AB-12 or MDA-MB-231 cells (10^6 cells in 100 μl of sterile PBS) and the tumors were allowed to form for 3–4 weeks. Tc99m-medronate was then injected into the tail veins of the mice (~800–1000 μCi per mouse) in 100 μl. High-resolution pinhole SPECT/CT imaging studies (X-SPECT system, GammaMedica, Inc., Northridge, CA) and biodistribution analyses were performed in nude mice with xenografted tumors to measure *in vivo* tumor retention of Tc99 medronate following i.v. injection. For SPECT imaging, a total of 64 projections were acquired with a 30-s acquisition time per projection, using a pinhole collimator with a 1-mm tungsten pinhole insert. Images were reconstructed using an ordered subsets expectation maximization (OSEM) algorithm with 20 iterations. In the CT system, the X-ray tube was operated at a voltage of 50 kV and an anode current of 0.6 mA. 256 projections were acquired to obtain the CT images, and acquisition time per projection was 0.5 s. The reconstructed images are 3 orientations with 1 mm mouse slices from the CT, SPECT, and fused SPECT/CT. The mice were terminated after imaging and tissues were collected and weighed ~8 h after injection with the Tc99m-medronate. The dose retention, or % Injected Dose per gram, (%ID/g) of each tissue was calculated by measuring the radioactivity in the tissue using a gamma counter, decay correcting the count rate data to the Tc99m-medronate injection time and normalizing to the total injected

dose in the animal as well as the tissue weight. Each animal's dose was determined by measuring the dosing syringe (AtomLab 100 dose calibrator) before and after injecting the mouse. To compare the accumulation of %ID/g between the breast cancer and mesothelioma-bearing mice, the %ID/g of the target tissue (subcutaneous tumor, femoral bone, heart muscle) was normalized against the %ID/g blood for each mouse. All animal studies were done in accordance with the local IACUC requirements. Also, the European Community guidelines for the use of experimental animals were adhered to.

2.9. Von Kossa staining to detect calcium deposits in mesothelioma and breast cancer tumors

To detect calcium minerals in the subcutaneously formed AB-12 and MDA-MB-231 tumors, they were first fixed in 10% neutral buffered formalin for 24 h and prepared into routine paraffin blocks. Sections of 5 μm in thickness were cut with a microtome. The sections were deparaffinized and hydrated through descending series of alcohol. The sections were placed in 5% silver nitrate solution and exposed to sunlight for 45 min, followed by 3 changes in deionized water. The sections were then treated in 2.5% sodium thiosulphate for 1 min, rinsed well in deionized water, dipped for 3.5 s in 0.5% gold chloride and rinsed well in deionized water. The sections were counterstained with Van Gieson's Picro-fuchsin for 5 min, and finally dehydrated, cleared and mounted. Chemically cleaned and well rinsed glassware was used throughout the staining procedure. With this staining, calcium deposits are seen as dark brown to black precipitations.

2.10. Statistical analysis

All results are expressed as the mean ± S.D., unless otherwise stated. Data were analyzed by Student's *t*-test. *P* values of <0.05 were considered significant.

3. Results

3.1. Excess pyrophosphate-resembling bisphosphonates antagonize nitrogen-containing bisphosphonate-induced accumulation of unprenylated Rap1A

We have shown previously that nitrogen-containing bisphosphonates induce a dose-dependent accumulation of unprenylated Rap1A in MDA-MB-231 (Merrell et al. manuscript submitted) and in AB-12 cells (Wakchoure et al., 2006). This effect of nitrogen-containing bisphosphonates can be reversed by excess geranylgeraniol, suggesting that it is mediated via inhibition of the mevalonate pathway (Wakchoure et al., 2006). It was recently shown that in macrophages, nitrogen-containing bisphosphonate-induced accumulation of unprenylated Rap1A could also be blocked with excess pyrophosphate-resembling bisphosphonates, which do not affect the mevalonate pathway, suggesting a presence of a cellular transporter of bisphosphonates for which the different classes of bisphosphonate molecules compete (Frith and Rogers, 2003). To investigate if a similar phenomenon can also be seen in cancer cells, we cultured MDA-MB-231 breast cancer and AB-12 mesothelioma cells with various concentrations of nitrogen-containing bisphosphonates (risedronate, zoledronate or alendronate) in the presence or absence of 10–1000 fold excess clodronate or etidronate for 24 h. The prenylation status of Rap1A in the cell lysates was studied with Western blots. As expected, clodronate or etidronate had no effect, but all the studied nitrogen-containing bisphosphonates induced a dose-dependent accumulation of unprenylated Rap1A. Zoledronate was the strongest inducer of this effect in both cell lines. In AB-12 cells the nitrogen-containing bisphosphonate-induced accumulation of unprenylated Rap1A was completely or partially reversed with both studied pyrophosphate-resembling bisphosphonates, depending on the concentration and the actual nitrogen-containing bisphosphonate that they were competed against (Fig. 1A). For example, when the pyrophosphate-resembling bisphosphonate: nitrogen-containing bisphosphonate ratio was 100:1, clodronate and etidronate completely blocked accumulation of unprenylated Rap1A induced by all nitrogen-

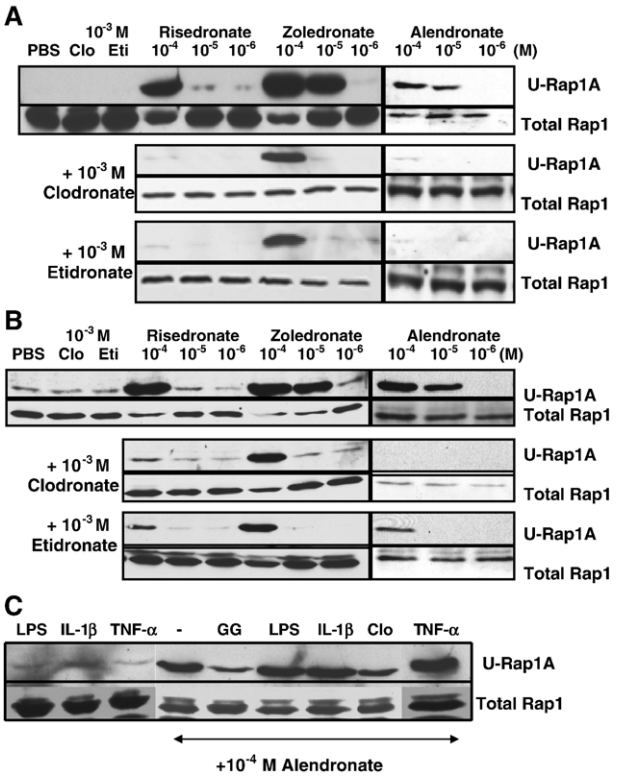

Fig. 1. Pyrophosphate-resembling bisphosphonates prevent the nitrogen-containing bisphosphonate-induced accumulation of unprenylated Rap1A in breast cancer and mesothelioma cells. A) AB-12 and B) MDA-MB-231 cells were treated for 24 h with PBS as a vehicle control or with the indicated concentrations of the various bisphosphonates, alone or in combination. Expression of unprenylated Rap1A (u-Rap1A, upper panels) and after stripping and re-blotting, total Rap1 (lower panels) were detected in Western blots, using antibodies that detect different forms of the protein. C) MDA-MB-231 cells were also treated with 10 ng/ml of LPS, IL-1β, TNF-α alone or with 10^{-4} M alendronate in combination with the indicated cytokines or LPS, clodronate (clo, 10^{-3} M) or geranylgeraniol (GG, 25 μM) for 24 h. Prenylation status of Rap1A was detected as above.

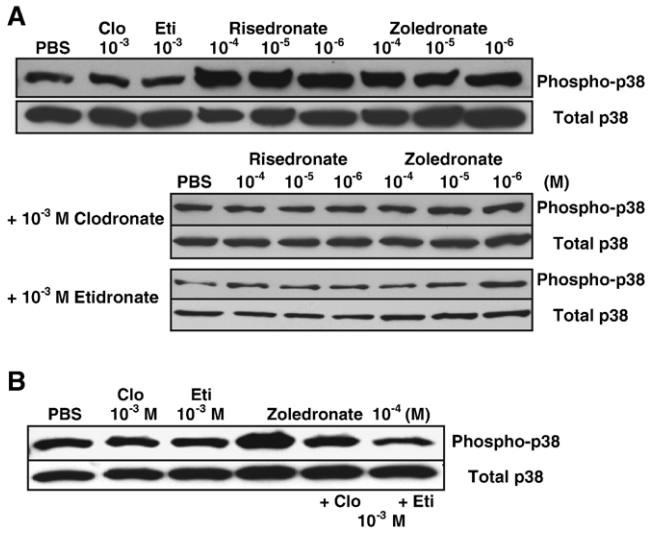

Fig. 2. Pyrophosphate-resembling bisphosphonates prevent the nitrogen-containing bisphosphonate-induced phosphorylation of p38 in cancer cells. A) AB-12 and B) MDA-MB-231 breast cancer cells were treated for 24 h with PBS as a vehicle control or with the indicated concentrations of the various bisphosphonates, alone or in combination with clodronate (clo, 10^{-3} M) or etidronate (eti, 10^{-3} M) for 24 h. The phosphorylation status of p38 was studied in Western blots, using phospho-p38 (upper panels) and total p38 (lower panels) specific antibodies.

containing bisphosphonates. Similar results were seen with MDA-MB-231 cells (Fig. 1B). For comparison, in addition to excess clodronate, alendronate-induced accumulation of unprenylated Rap1A in MDA-MB-231 cells was reduced only with the addition of excess geranylgeraniol (25 μM), but it was not blocked with TNF-α, IL-1β or LPS which are completely unrelated molecules to bisphosphonates (Fig. 1C).

3.2. Excess pyrophosphate-resembling bisphosphonates antagonize nitrogen-containing bisphosphonate-induced phosphorylation of p38

We have shown previously that treatment with nitrogen-containing bisphosphonates induces the phosphorylation of the p38 MAP kinase in macrophages and in breast cancer and mesothelioma cells (Merrell et al., 2003; Wakchoure et al., 2006). This effect signals for resistance against the growth inhibitory effects of these drugs and is independent of the nitrogen-containing bisphosphonate-induced inhibition of the mevalonate pathway (Merrell et al., 2003; Wakchoure et al.,

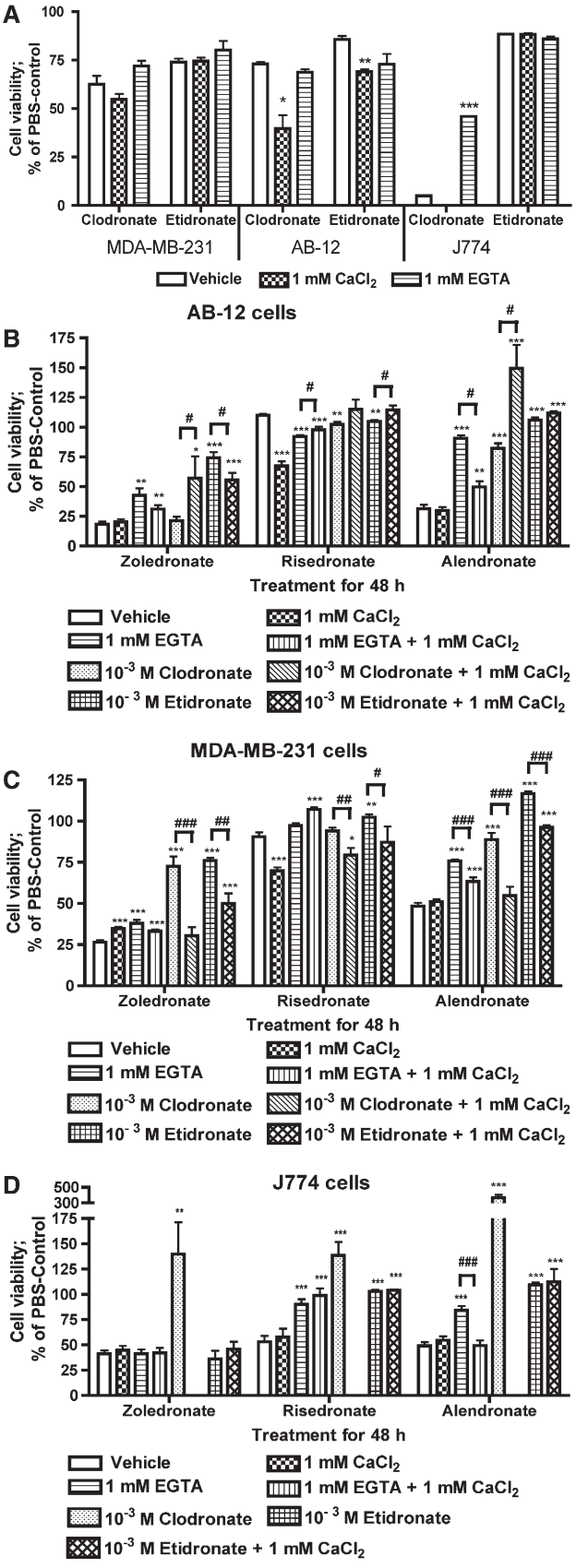

Fig. 3. Pyrophosphate-resembling bisphosphonates prevent the growth inhibitory effects of nitrogen-containing bisphosphonates in cancer cells. A) The indicated cells were treated with PBS or 10^{-3} M clodronate or etidronate, with or without vehicle, 1 mM $CaCl_2$ or 1 mM EGTA for 72 h and viability was measured with MTS-assays. Data is expressed as % of PBS-control in the corresponding groups. Mean±S.D., $n=10–15$. * $P<0.05$, ** $P<0.01$, *** $P<0.001$ vs. vehicle-treated group. B) AB-12, C) MDA-MB-231 or D) J774 cells were treated with PBS or with the indicated nitrogen-containing bisphosphonates (zoledronate, risedronate, alendronate), in combination with vehicle, 1 mM $CaCl_2$, 1 mM EGTA, 1 mM EGTA+1 mM $CaCl_2$, or with 10^{-3} M pyrophosphate-resembling bisphosphonates (clodronate or etidronate), with or without 1 mM $CaCl_2$. Cell viability was measured 72 h later with MTS-assays. Data is expressed as % of corresponding PBS-control for each treatment, mean±S.D., $n=15–20$, * $P<0.05$, ** $P<0.01$, *** $P<0.001$ vs. corresponding vehicle-treatment group. # $P<0.05$, ## $P<0.01$, ### $P<0.001$ vs. corresponding treatment containing Ca^{2+}.

2006). We therefore studied the combined effects of nitrogen-containing bisphosphonates and pyrophosphate-resembling bisphosphonates also on p38 activation. Unlike shown earlier with lower (10^{-5} M) concentrations (Merrell et al., 2003), the high (10^{-3} M) concentrations of pyrophosphate-resembling bisphosphonates used here did not induce phosphorylation of p38 in either studied cell line. All studied nitrogen-containing bisphosphonates (10^{-4}–10^{-6} M) did, however, induce p38 phosphorylation in AB-12 cells. Addition of excess clodronate or etidronate simultaneously with the nitrogen-containing bisphosphonates (risedronate or zoledronate) blocked this effect (Fig. 2A). Similar results were seen also in MDA-MB-231 cells where zoledronate-induced (10^{-4} M) p38 phosphorylation was blocked with both clodronate and etidronate (10^{-3} M) (Fig. 2B).

3.3. Excess pyrophosphate-resembling bisphosphonates antagonize the growth inhibitory effects of nitrogen-containing bisphosphonates

We next studied whether the pyrophosphate-resembling bisphosphonates affect the growth inhibitory effects of nitrogen-containing bisphosphonates. To do this, we first assessed the effects of the high pyrophosphate-resembling bisphosphonate doses (10^{-3} M) alone or in combination with 1 mM EGTA or Ca^{2+} on the viability of MDA-MB-23, AB-12 or J774 cells. The macrophage-like J774 cells were included in these studies, because it has been previously reported that Ca^{2+} and EGTA in the culture medium affect bisphosphonate uptake in these cells (Mönkkönen et al., 1994; Pennanen et al., 1995; Thompson et al., 2006a). The high doses of pyrophosphate-resembling bisphosphonates alone decreased the viability of all studied cells ($P<0.001$ vs. corresponding PBS-control). The J774 macrophage-like cells exhibited the highest sensitivity to the growth inhibitory effects of clodronate, which was reversed by addition of 1 mM EGTA. Addition of 1 mM $CaCl_2$ did not affect the growth inhibitory effects of pyrophosphate-resembling bisphosphonates in MDA-MB-231 cells, but enhanced those in AB-12 cells. The combination of clodronate and 1 mM $CaCl_2$ was toxic to J774 cells. Otherwise, addition of EGTA or $CaCl_2$ did not interfere with pyrophosphate-resembling bisphosphonate effects on viability in these cell lines (Fig. 3A). We next assessed whether excess (10^{-3} M) pyrophosphate-resembling bisphosphonates (clodronate or etidronate) affect the cell viability changes induced by 10^{-4} M nitrogen-containing bisphosphonates (alendronate, risedronate or zoledronate). All nitrogen-containing bisphosphonates, except for risedronate, induced a significant decrease in cell viability ($P<0.001$) in MDA-MB-231 and AB-12 cells. In J774 cells, also risedronate significantly decreased cellular viability. The obvious growth inhibitory effects of the nitrogen-containing bisphosphonates were reversed by pyrophosphate-resembling bisphosphonates. There were, however, cell- and drug-specific exceptions to these results. The growth inhibitory effects of zoledronate were not reversed by clodronate in AB-12 and by etidronate in J774 cells. There were also differences in cellular responses to the combination of risedronate and pyrophosphate-resembling bisphosphonates; Clodronate decreased slightly, but significantly cell viability when these two drugs were given simultaneously to AB-12 cells, but it did not interfere with risedronate effects in MDA-MB-231 cells. In J774 cells, clodronate significantly reversed the risedronate-induced decrease in viability. When compared with vehicle + risedronate-treatment, etidronate + risedronate-treatment decreased cell viability in AB-12 cells but increased it in MDA-MB-231 cells. In J774 cells, etidronate reversed risedronate-induced decrease in viability (Fig. 3B–D). It was shown recently that cellular up-take of nitrogen-

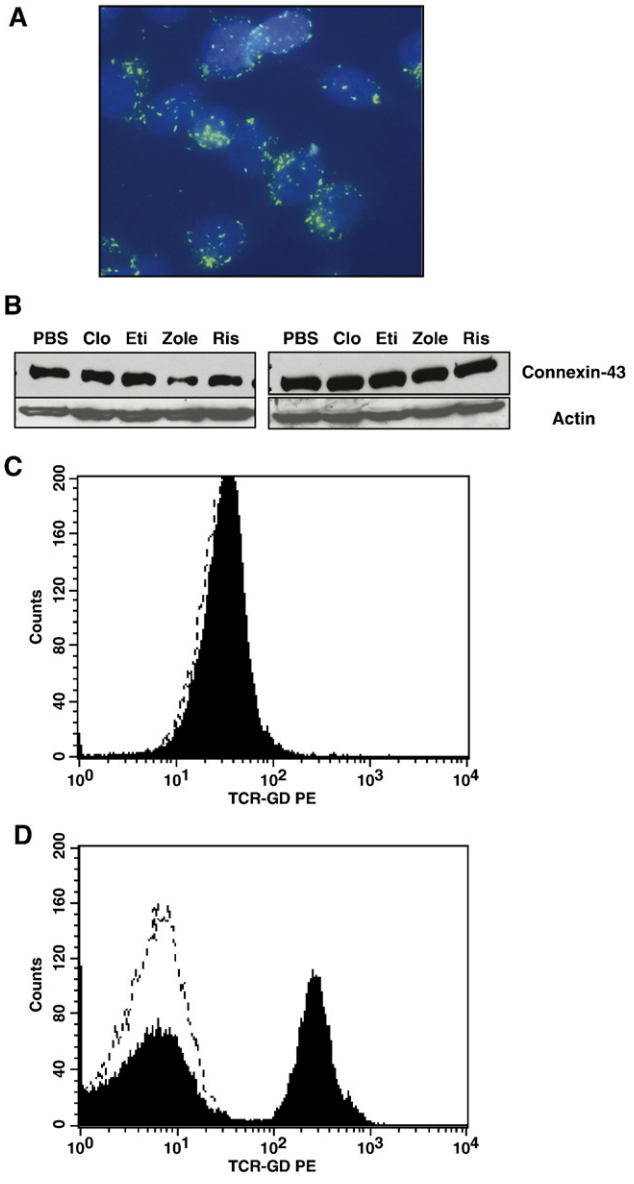

Fig. 4. MDA-MB-231 cells express connexin-43 but not γλ-TCR. A) Immunofluorescent detection of connexin-43 staining on the cell membrane of MDA-MB-231 cells. B) Western blots to show the effects of 24 h treatment with the indicated bisphosphonates on the expression of connexin-43 in MDA-MB-231 cells. The same blots were stripped and reblotted for actin, to show equal loading. Flow cytometry analysis of γλ-T-cell receptor in C) MDA-MB-231 and D) in cultured human mononuclear cells as a positive staining control. PE-conjugated anti-γλ-TCR mAb is shown with solid black line and the PE-conjugated isotypic control mAb with a dashed line.

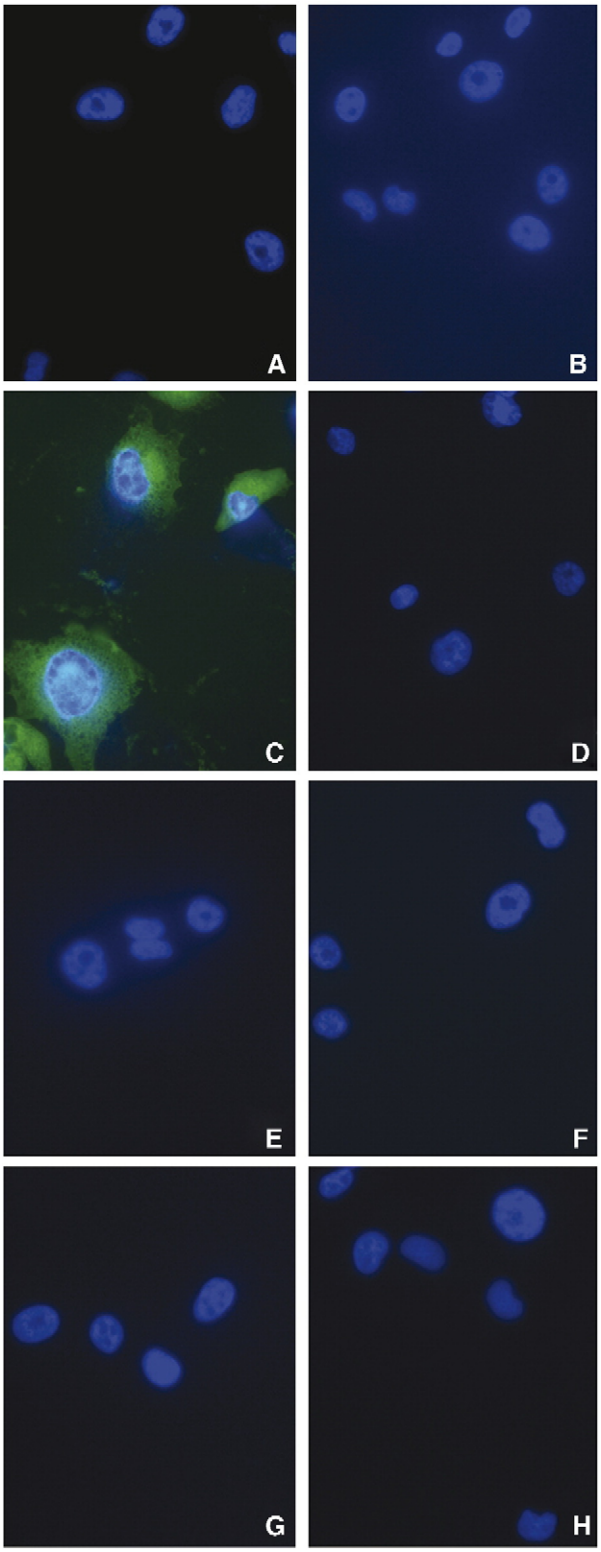

Fig. 5. Nitrogen-containing bisphosphonates do not mediate Lucifer yellow uptake in MDA-MB-231 cells. The cells were cultured for 15 min in the presence of A) vehicle, B) heptanol, C) EGTA, D) heptanol+EGTA, E) alendronate, F) heptanol+alendronate, G) zoledronate or H) with heptanol+zoledronate. The effects on Luciferase yellow uptake were followed with a fluorescent microscope.

containing bisphosphonates in macrophages is increased by adding excess Ca^{2+} to the culture medium and that the antagonistic effects of pyrophosphate-resembling bisphosphonates against nitrogen-containing bisphosphonates are similar to those of EGTA and due to Ca^{2+}-chelation (Thompson et al., 2006a). We therefore investigated whether manipulating culture medium Ca^{2+} concentrations affects the ability of pyrophosphate-resembling bisphosphonates to antagonize the effects of nitrogen-containing bisphosphonates on cellular viability. The results again were bisphosphonate- and cell-specific. Addition of Ca^{2+} slightly reversed the growth inhibitory effects of

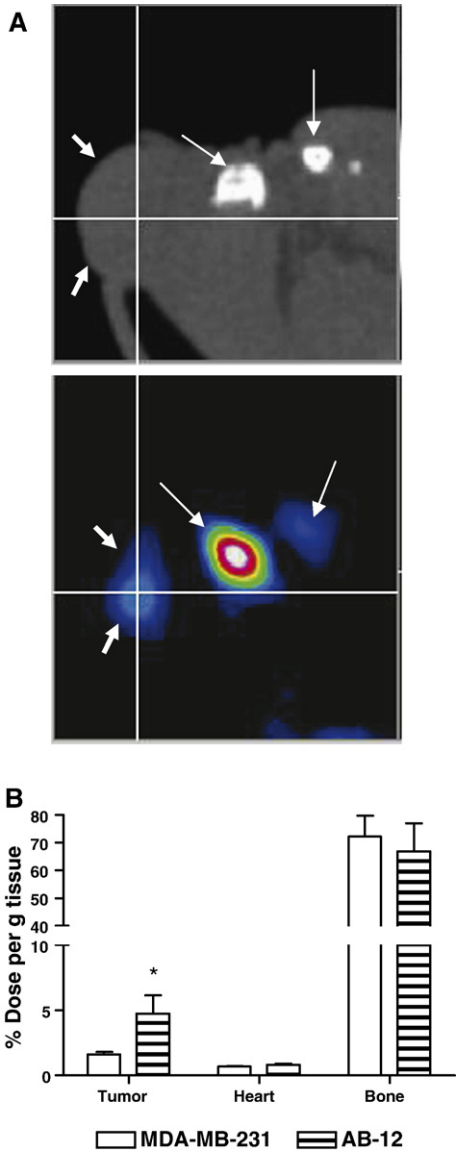

Fig. 6. Mesothelioma tumors exhibit higher Tc99m-medronate uptake than breast cancer tumors. A) Accumulation of Tc99m-medronate was detected in bones (long arrows), as well as in the subcutaneous tumors (short arrows) in both AB-12 and MDA-MB-231 bearing mice. The pictures represent CT-(upper panel) and SPECT-(lower panel) images of an AB-12 tumor bearing mouse. (B) The % dose retention in the indicated target tissues of MDA-MB-231 or AB-12 tumor bearing mice. Mean±S.D., $n=10–15$ indicating the number of tissues analyzed. * $P<0.05$ vs. the MDA-MB-231 tumor.

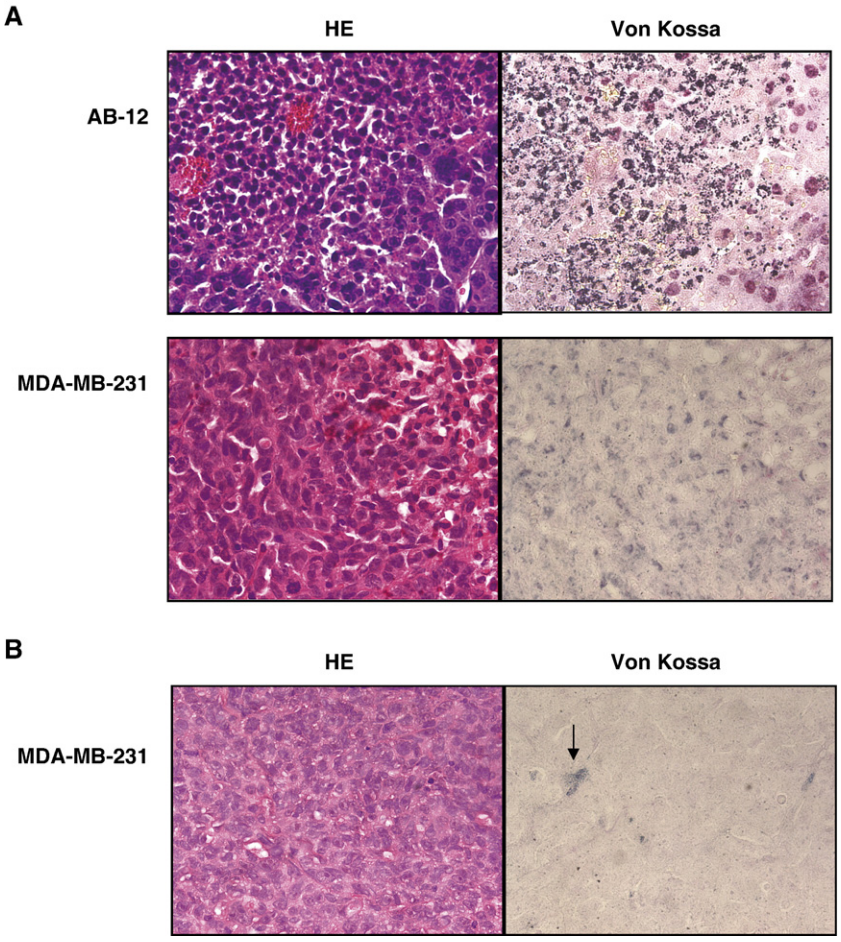

Fig. 7. Mesothelioma and breast tumors exhibit calcification. A) H and E (left panels) and Von Kossa stainings (right panels) of AB-12 and MDA-MB-231 tumors. Intracellular staining is seen in AB-12 cells in areas of necrosis. In tumors formed by MDA-MB-231 cells, also cells within the vicinity of necrotic cells exhibit positive staining. B) For comparison, viable tumor is shown, with positive staining in only 2 cells (arrows).

zoledronate in MDA-MB-231 cells and enhanced the growth inhibitory effects of risedronate in both cancer cell lines. Surprisingly, in J774 cells, excess Ca^{2+} did not augment the nitrogen-containing bisphosphonate effects on viability. Addition of EGTA reversed zoledronate- and alendronate-induced growth inhibition in both cancer cell lines and enhanced the growth inhibitory effects of risedronate in AB-12 cells. In J774 cells, EGTA reversed the growth inhibitory effects of risedronate and alendronate. Excess Ca^{2+} significantly decreased the EGTA effect in reversing alendronate-induced growth inhibition of all three cell lines. Although the same was seen in the zoledronate-group in the cancer cell lines, the effects were not statistically significant. Excess Ca^{2+} also reversed the ability of EGTA to potentiate risedronate-induced growth inhibitory effects in AB-12 cells. In MDA-MB-231 cells, simultaneous addition of Ca^{2+} with EGTA increased viability in the risedronate-group, as compared with the corresponding risedronate + vehicle-treated control. Addition of 1 mM $CaCl_2$ simultaneously with clodronate or etidronate decreased the ability of these pyrophosphate-resembling bisphosphonates to protect against nitrogen-containing bisphosphonate-induced decrease in viability in MDA-MB-231 cells. The results were the opposite with clodronate and Ca^{2+} in AB-12 cells, where Ca^{2+} potentiated the protective effects of clodronate against zoledronate and alendronate. Similar effects were also seen with etidronate and Ca^{2+} in the risedronate-group in AB-12 cells. Addition of excess Ca^{2+}, however, either significantly decreased or did not interfere with the protective effect of etidronate against zoledronate or alendronate, respectively, in the AB-12 cells. In J774 cells, etidronate effects against nitrogen-containing bisphosphonates were not affected by Ca^{2+} and the presence of clodronate with Ca^{2+} was toxic in all treatment groups (Fig. 3B – D).

3.4. Treatment with nitrogen-containing bisphosphonates does not increase hemichannel mediated uptake in MDA-MB-231 cells

Other proteins through which the cellular effects of bisphosphonates have been shown to be mediated include the connexin-43 hemichannel and γλTCR (Plotkin et al., 2005; Plotkin and Bellido, 2001; Thompson and Rogers, 2004; Thompson et al., 2006b). More specifically, nitrogen-containing bisphosphonates were shown to open connexin-43 hemichannels, resulting in the activation of the Scr and ERK kinases and increased cell survival of osteocytes (Plotkin et al., 2005, 2002; Plotkin and Bellido, 2001). To investigate the possibility that

similar mechanisms might operate also in cancer, we first analyzed the expression of these proteins in MDA-MB-231 cells. γλTCR expression was detected with Flow cytometry in peripheral blood monocytes, but not in MDA-MB-231 cells. Connexin-43 expression was seen on the cell membranes of MDA-MB-231 cells using immunofluorescence. Treatment for 24 h with zoledronate (10^{-4} M), but not with any other tested bisphosphonate, slightly decreased the connexin-43 expression (Fig. 4). Treatment of the MDA-MB-231 cells with EGTA increased the uptake of Luciferin yellow from the surrounding culture medium, and this was preventable with heptanol, suggesting that the connexin-43 mediated uptake is functional in these cells. Nitrogen-containing bisphosphonates did not, however, increase the uptake of Luciferin yellow in these cells (Fig. 5).

3.5. Mesothelioma tumors exhibit higher Tc99m-medronate uptake than breast cancer tumors

To investigate bisphosphonate uptake into tumors *in vivo*, we inoculated MDA-MB-231 and AB-12 cells subcutaneously into nude mice and allowed tumors to form. The animals were then injected with the bone scanning agent Tc99m-medronate and the % dose retention was analyzed in various tissues. As expected, the highest proportion of the drug accumulated in the bones. Furthermore, as expected, accumulation of radioactivity was similar in the hearts and femoral bones in both groups of mice that were bearing either breast cancer or mesothelioma tumors. Accumulation of Tc99m-medronate was, however, significantly higher in the mesothelioma tumors formed by the AB-12 cells, as compared with breast cancer tumors formed by the MDA-MB-231 cells (Fig. 6). Finally, to begin to investigate the mechanisms through which the bone scanning agent is retained within the tumors, we analyzed them with Von Kossa-stainings which detect Ca^{2+}-minerals. In both tumor types, patchy, intracellular positive staining for Ca^{2+}-minerals was detected. In the mesothelioma tumors, staining was only seen in areas of tumor necrosis. In breast cancer tumors, cells surrounding necrotic areas stained positive with Von Kossa. No positive staining was seen in areas of viable tumors formed by AB-12 cells and only rarely in individual cells of viable tumors formed by MDA-MB-231 cells (Fig. 7).

4. Discussion

With increasing clinical evidence suggesting beneficial effects of bisphosphonate-treatment in cancer, it is likely that the use of these drugs in oncology will increase (Diel et al., 1998; Powles et al., 2006, 2002). Some of the main remaining questions are whether or not bisphosphonates gain access into tumor cells that are growing at the soft-tissue sites and if so, what are the direct effects of bisphosphonates in these cells. Furthermore, it is not known why certain tumors appear to be more sensitive to the anti-cancer effects of bisphosphonates than others, as seen in various animal models of cancer (Hashimoto et al., 2005; Hiraga et al., 2001; Ory et al., 2005; Wakchoure et al., 2006).

We compared the effects of bisphosphonates in mesothelioma and breast cancer cells, which have been shown to exhibit different sensitivities to the growth inhibitory effects of bisphosphonates *in vivo* (Hiraga et al., 2001; Sasaki et al., 1995; Wakchoure et al., 2006). We show here for the first time that accumulation of Tc99m-medronate, a bisphosphonate that is clinically used in bone scans, is significantly higher in subcutaneous mesothelioma tumors, as compared with subcutaneous breast tumors. Although accumulation of medronate cannot be considered to represent the accumulation of all bisphosphonates into tumors at the soft tissue sites, these findings do suggest that the increased sensitivity of mesothelioma cells to the growth inhibitory effects of bisphosphonates *in vivo*, may be related to their increased intratumoral accumulation of these drugs (Hiraga et al., 2001, 2004; Wakchoure et al., 2006).

The mechanisms of intratumoral accumulation of bisphosphonates is not understood. It was shown recently that pyrophosphate-resembling bisphosphonates block the cell biological effects of nitrogen-containing bisphosphonates in osteoclasts and macrophages. This phenomenon was initially thought to represent a competition of the two groups of bisphosphonates for a specific up-take mechanisms in cells (Frith and Rogers, 2003). Recent results by Thompson et al. (2006a), however, suggest that the antagonistic effects of pyrophosphate-resembling bisphosphonates against nitrogen-containing bisphosphonates are due to the calcium-chelating effects of the excess pyrophosphate-resembling bisphosphonates present in the experimental setting, at least in macrophages (Thompson et al., 2006a). We show here that pyrophosphate-containing bisphosphonates can block nitrogen-containing bisphosphonate-induced effects also in breast cancer and mesothelioma cells. We further show that the effects of bisphosphonates on cellular viability can be regulated by affecting the culture medium Ca^{2+}-concentration. There are, however, significant cell and drug-specific differences in how cells respond to the combination of bisphosphonates and Ca^{2+}. For example, our results show that excess Ca^{2+} reverses the ability of zoledronate to decrease viability in MDA-MB-231 breast cancer cells, but not in AB-12 mesothelioma cells. Also, addition of Ca^{2+} augmented the growth inhibitory effects of clodronate and etidronate in AB-12 cells, but not in MDA-MB-231 cells. Our results agree with those of Thompson et al., 2006a, which suggested that the antagonistic effects of excess pyrophosphate-resembling bisphosphonates against nitrogen-containing bisphosphonates may be explained by their ability to chelate calcium, resulting in decreased cellular up-take of nitrogen-containing bisphosphonates, which is Ca^{2+} dependent. However, this does not appear to be always the case because for example in AB-12 and J774 cells, we were unable to reverse the protective effects of etidronate against alendronate with excess Ca^{2+}. Therefore, our results still leave open the possibility that there is a step or steps during the intracellular processing of bisphosphonates for which the various drug molecules compete. Unexpectedly also, even though increased Ca^{2+} in the culture medium was shown to increase J774 uptake of nitrogen-containing

bisphosphonates (Thompson et al., 2006a), we still did not observe changes in J774 viability when the cells were cultured with excess Ca^{2+} and nitrogen-containing bisphosphonates, as compared with treatment with nitrogen-containing bisphosphonates alone. The only situation where excess Ca^{2+} augmented the nitrogen-containing bisphosphonate-induced decrease in cellular viability was seen with risedronate in the cancer cells studied here. The reason for these discrepancies are currently not known. Taken together, these observations suggest that the combination of extracellular Ca^{2+} and bisphosphonates may have cell and drug molecule specific effects on cell viability. These findings may have clinical relevance because, as shown here with Von Kossa stainings, and as also seen in clinical specimens, calcification is a well known feature in breast carcinomas and has also been detected in malignant mesotheliomas (Morgan et al., 2005; Nichols and Johnson, 1983; Raizon et al., 1996). Whether or not differences in tumor calcification explain differences to *in vivo* sensitivity to bisphosphonates requires further study.

At least two additional mechanisms have been shown to mediate the cellular effects of bisphosphonates. Connexin-43 was shown to mediate the anti-apoptotic effects of alendronate in MLO-Y4 osteocyte-like cells (Plotkin and Bellido, 2001). Nitrogen-containing bisphosphonates have also been shown to affect cells via the γλT-cell receptor (Sato et al., 2005; Thompson and Rogers, 2004; Thompson et al., 2006b). MDA-MB-231 breast cancer cells express connexin-43 on their cell membranes, as shown here and also previously (Shao et al., 2005). Treatment with a high dose of zoledronate for 24 h appeared to slightly decrease the expression of connexin-43, but we did not detect increased hemichannel-mediated cellular uptake of Lucifer yellow in response to short-term alendronate or zoledronate-treatment. These results suggests that the nitrogen-containing bisphosphonate effects on hemichannels are cell-specific and do not necessarily occur in breast cancer cells. We did not detect γλT-cell receptor expression in these breast cancer cells either, suggesting that nitrogen-containing bisphosphonates do not affect MDA-MB-231 breast cancer cells via this receptor.

In conclusion, we show here that mesothelioma cells have a higher capacity to accumulate the bone scanning bisphosphonate *in vivo*. The cellular effects of nitrogen-containing bisphosphonates can be overcome by excess pyrophosphate-resembling bisphosphonates in both mesothelioma and breast cancer cells. Part of this may be explained by Ca^{2+}-chelation by the pyrophosphate-resembling bisphosphonates, and thereby, decreased cellular up-take of the nitrogen-containing bisphosphonates. It is, however, possible that there are additional steps in the intracellular processing of these drugs for which the different molecules compete. Our results further suggest that the cancer growth inhibiting effects of bisphosphonates may be affected by extracellular Ca^{2+} in a cancer cell- and bisphosphonate-specific fashion. Since calcifications are frequently seen in malignant tumors, it is possible that tumor calcification also affects the outcomes of bisphosphonate-treatment in tumors that are growing at visceral sites.

Acknowledgements

This work was supported by UAB Comprehensive Cancer Center Mesothelioma grant (K.S.S.), and by Department of Defense (W81XWH-04-1-0479, K.S.S).

References

Alakangas, A., Selander, K., Mulari, M., Halleen, J., Lehenkari, P., Mönkkönen, J., Salo, J., Väänänen, H.K., 2002. Alendronate disturbs vesicular trafficking in osteoclasts. Calcif. Tissue Int. 70, 40–47.

Barai, S., Kumar, R., Haloi, A.K., Dhanpati, Banopadhyaya, G., Malhotra, A., 2004. Bone scan demonstrating metastasis to the breast from an ovarian carcinoma and a review of the literature. Clin. Nucl. Med. 29, 167–170.

Beres, R.A., Patel, N., Krasnow, A.Z., Isitman, A.T., Hellman, R.S., Veluvolu, P., Patillo, R.S., Collier, B.D., 1991. Concentration of Tc-99m MDP in ovarian carcinoma and its soft tissue metastases. Clin. Nucl. Med. 16, 550–552.

Chuah, C., Barnes, D.J., Kwok, M., Corbin, A., Deininger, M.W., Druker, B.J., Melo, J.V., 2005. Zoledronate inhibits proliferation and induces apoptosis of imatinib-resistant chronic myeloid leukaemia cells. Leukemia 19, 1896–1904.

Coxon, F.P., Helfrich, M.H., van't Hof, R., Sebti, S., Ralston, S.H., Hamilton, A., Rogers, M.J., 2000. Protein geranylgeranylation is required for osteoclast formation, function, and survival: inhibition by bisphosphonates and GGTI-298. J. Bone Miner. Res. 15, 1467–1476.

Diel, I.J., Solomayer, E.F., Costa, S.D., Gollan, C., Goerner, R., Wallwiener, D., Kaufmann, M., Bastert, G., 1998. Reduction in new metastases in breast cancer with adjuvant clodronate treatment. N. Engl. J. Med. 339, 357–363.

Fogelman, I., Bessent, R.G., Turner, J.G., Citrin, D.L., Boyle, I.T., Greig, W.R., 1978. The use of whole-body retention of Tc-99m diphosphonate in the diagnosis of metabolic bone disease. J. Nucl. Med. 19, 270–275.

Frith, J.C., Rogers, M.J., 2003. Antagonistic effects of different classes of bisphosphonates in osteoclasts and macrophages in vitro. J. Bone Miner. Res. 18, 204–212.

Hashimoto, K., Morishige, K., Sawada, K., Tahara, M., Kawagishi, R., Ikebuchi, Y., Sakata, M., Tasaka, K., Murata, Y., 2005. Alendronate inhibits intraperitoneal dissemination in in vivo ovarian cancer model. Cancer Res. 65, 540–545.

Hiraga, T., Williams, P.J., Mundy, G.R., Yoneda, T., 2001. The bisphosphonate ibandronate promotes apoptosis in MDA-MB-231 human breast cancer cells in bone metastases. Cancer Res. 61, 4418–4424.

Hiraga, T., Williams, P.J., Ueda, A., Tamura, D., Yoneda, T., 2004. Zoledronic acid inhibits visceral metastases in the 4T1/luc mouse breast cancer model. Clin. Cancer Res. 10, 4559–4567.

Hosfield, D.J., Zhang, Y., Dougan, D.R., Broun, A., Tari, L.W., Swanson, R.V., Finn, J., 2004. Structural basis for bisphosphonate-mediated inhibition of isoprenoid biosynthesis. J. Biol. Chem. 279, 8526–8529.

Iguchi, T., Miyakawa, Y., Yamamoto, K., Kizaki, M., Ikeda, Y., 2003. Nitrogen-containing bisphosphonates induce S-phase cell cycle arrest and apoptosis of myeloma cells by activating MAPK pathway and inhibiting mevalonate pathway. Cell. Signal. 15, 719–727.

Lehenkari, P.P., Kellinsalmi, M., Näpänkangas, J.P., Ylitalo, K.V., Mönkkönen, J., Rogers, M.J., Azhayev, A., Väänänen, H.K., Hassinen, I.E., 2002. Further insight into mechanism of action of clodronate: inhibition of mitochondrial ADP/ATP translocase by a nonhydrolyzable, adenine-containing metabolite. Mol. Pharmacol. 61, 1255–1262.

Matsumoto, S., Kimura, S., Segawa, H., Kuroda, J., Yuasa, T., Sato, K., Nogawa, M., Tanaka, F., Maekawa, T., Wada, H., 2005. Efficacy of the third-generation bisphosphonate, zoledronic acid alone and combined with anti-cancer agents against small cell lung cancer cell lines. Lung Cancer 47, 31–39.

Merrell, M., Suarez-Cuervo, C., Harris, K.W., Väänänen, H.K., Selander, K.S., 2003. Bisphosphonate induced growth inhibition of breast cancer cells is augmented by p38 inhibition. Breast Cancer Res. Treat. 81, 231–241.

Mönkkönen, J., Taskinen, M., Auriola, S.O., Urtti, A., 1994. Growth inhibition of macrophage-like and other cell types by liposome-encapsulated, calcium-bound, and free bisphosphonates in vitro. J. Drug Target. 2, 299–308.

Mönkkönen, H., Auriola, S., Lehenkari, P., Kellinsalmi, M., Hassinen, I.E., Vepsäläinen, J., Mönkkönen, J., 2006. A new endogenous ATP analog (ApppI) inhibits the mitochondrial adenine nucleotide translocase (ANT) and is responsible for the apoptosis induced by nitrogen-containing bisphosphonates. Br. J. Pharmacol. 147, 437–445.

Morgan, M.P., Cooke, M.M., McCarthy, G.M., 2005. Microcalcifications associated with breast cancer: an epiphenomenon or biologically significant feature of selected tumors? J. Mammary Gland Biol. Neoplasia 10, 181–187.

Nichols, D.M., Johnson, M.A., 1983. Calcification in a pleural mesothelioma. J. Can. Assoc. Radiol. 34, 311–313.

Ory, B., Heymann, M.F., Kamijo, A., Gouin, F., Heymann, D., Redini, F., 2005. Zoledronic acid suppresses lung metastases and prolongs overall survival of osteosarcoma-bearing mice. Cancer 104, 2522–2529.

Pennanen, N., Lapinjoki, S., Urtti, A., Mönkkönen, J., 1995. Effect of liposomal and free bisphosphonates on the IL-1 beta, IL-6 and TNF alpha secretion from RAW 264 cells in vitro. Pharm. Res. 12, 916–922.

Plotkin, L.I., Bellido, T., 2001. Bisphosphonate-induced, hemichannel-mediated, anti-apoptosis through the Src/ERK pathway: a gap junction-independent action of connexin-43. Cell Commun. Adhes. 8, 377–382.

Plotkin, L.I., Manolagas, S.C., Bellido, T., 2002. Transduction of cell survival signals by connexin-43 hemichannels. J. Biol. Chem. 277, 8648–8657.

Plotkin, L.I., Aguirre, J.I., Kousteni, S., Manolagas, S.C., Bellido, T., 2005. Bisphosphonates and estrogens inhibit osteocyte apoptosis via distinct molecular mechanisms downstream of extracellular signal-regulated kinase activation. J. Biol. Chem. 280, 7317–7325.

Powles, T., Paterson, S., Kanis, J.A., McCloskey, E., Ashley, S., Tidy, A., Rosenqvist, K., Smith, I., Ottestad, L., Legault, S., Pajunen, M., Nevantaus, A., Männistö, E., Suovuori, A., Atula, S., Nevalainen, J., Pylkkänen, L., 2002. Randomized, placebo-controlled trial of clodronate in patients with primary operable breast cancer. J. Clin. Oncol. 20, 3219–3224.

Powles, T., Paterson, A., McCloskey, E., Schein, P., Scheffler, B., Tidy, A., Ashley, S., Smith, I., Ottestad, L., Kanis, J., 2006. Reduction in bone relapse and improved survival with oral clodronate for adjuvant treatment of operable breast cancer [ISRCTN83688026]. Breast Cancer Res. 8, R13.

Raizon, A., Schwartz, A., Hix, W., Rockoff, S.D., 1996. Calcification as a sign of sarcomatous degeneration of malignant pleural mesotheliomas: a new CT finding. J. Comput. Assist. Tomogr. 20, 42–44.

Reinholz, G.G., Getz, B., Sanders, E.S., Karpeisky, M.Y., Padyukova, N., Mikhailov, S.N., Ingle, J.N., Spelsberg, T.C., 2002. Distinct mechanisms of bisphosphonate action between osteoblasts and breast cancer cells: identity of a potent new bisphosphonate analogue. Breast Cancer Res. Treat. 71, 257–268.

Riebeling, C., Forsea, A.M., Raisova, M., Orfanos, C.E., Geilen, C.C., 2002. The bisphosphonate pamidronate induces apoptosis in human melanoma cells in vitro. Br. J. Cancer 87, 366–371.

Rodan, G.A., Martin, T.J., 2000. Therapeutic approaches to bone diseases. Science 289, 1508–1514.

Rogers, M.J., 2004. From molds and macrophages to mevalonate: a decade of progress in understanding the molecular mode of action of bisphosphonates. Calcif. Tissue Int. 75, 451–461.

Saarto, T., Blomqvist, C., Virkkunen, P., Elomaa, I., 2001. Adjuvant clodronate treatment does not reduce the frequency of skeletal metastases in node-positive breast cancer patients: 5-year results of a randomized controlled trial. J. Clin. Oncol. 19, 10–17.

Sasaki, A., Boyce, B.F., Story, B., Wright, K.R., Chapman, M., Boyce, R., Mundy, G.R., Yoneda, T., 1995. Bisphosphonate risedronate reduces metastatic human breast cancer burden in bone in nude mice. Cancer Res. 55, 3551–3557.

Sato, K., Kimura, S., Segawa, H., Yokota, A., Matsumoto, S., Kuroda, J., Nogawa, M., Yuasa, T., Kiyono, Y., Wada, H., Maekawa, T., 2005. Cytotoxic effects of gammadelta T cells expanded ex vivo by a third generation bisphosphonate for cancer immunotherapy. Int. J. Cancer 116, 94–99.

Sawada, K., Morishige, K., Tahara, M., Kawagishi, R., Ikebuchi, Y., Tasaka, K., Murata, Y., 2002. Alendronate inhibits lysophosphatidic acid-induced migration of human ovarian cancer cells by attenuating the activation of rho. Cancer Res. 62, 6015–6020.

Selander, K.S., Mönkkönen, J., Karhukorpi, E.K., Härkönen, P., Hannuniemi, R., Väänänen, H.K., 1996. Characteristics of clodronate-induced apoptosis in osteoclasts and macrophages. Mol. Pharmacol. 50, 1127–1138.

Senaratne, S.G., Colston, K.W., 2002. Direct effects of bisphosphonates on breast cancer cells. Breast Cancer Res. 4, 18–23.

Shao, Q., Wang, H., McLachlan, E., Veitch, G.I., Laird, D.W., 2005. Down-regulation of Cx43 by retroviral delivery of small interfering RNA promotes an aggressive breast cancer cell phenotype. Cancer Res. 65, 2705–2711.

Skerjanec, A., Berenson, J., Hsu, C., Major, P., Miller Jr., W.H., Ravera, C., Schran, H., Seaman, J., Waldmeier, F., 2003. The pharmacokinetics and pharmacodynamics of zoledronic acid in cancer patients with varying degrees of renal function. J. Clin. Pharmacol. 43, 154–162.

Swayne, L.C., Hediger, R.G., Wolff, M., 1992. Bone scan detection of pelvic metastasis from pleural mesothelioma. Clin. Nucl. Med. 17, 965–966.

Tanabe, M., Mizukawa, K., Sugita, K., Tamai, T., Wakabayashi, H., Morino, Y., 1979. 99mTc-diphosphonate uptake in small cell carcinoma of the lung. Radioisotopes 28, 177–179.

Thompson, K., Rogers, M.J., 2004. Statins prevent bisphosphonate-induced gamma, delta-T-cell proliferation and activation in vitro. J. Bone Miner. Res. 19, 278–288.

Thompson, K., Rogers, M.J., Coxon, F.P., Crockett, J.C., 2006a. Cytosolic entry of bisphosphonate drugs requires acidification of vesicles following fluid-phase endocytosis. Mol. Pharmacol. 69, 1624–1632.

Thompson, K., Rojas-Navea, J., Rogers, M.J., 2006b. Alkylamines cause Vgamma9Vdelta2 T-cell activation and proliferation by inhibiting the mevalonate pathway. Blood 107, 651–654.

van Beek, E., Pieterman, E., Cohen, L., Löwik, C., Papapoulos, S., 1999. Farnesyl pyrophosphate synthase is the molecular target of nitrogen-containing bisphosphonates. Biochem. Biophys. Res. Commun. 264, 108–111.

Vorne, M., Saukko, T., 1984. Detection of malignant soft tissue tumors in bone imaging. Eur. J. Nucl. Med. 9, 180–184.

Wakchoure, S., Merrell, M.A., Aldrich, W., Millender-Swain, T., Harris, K.W., Triozzi, P., Selander, K.S., 2006. Bisphosphonates inhibit the growth of mesothelioma cells in vitro and in vivo. Clin. Cancer Res. 12, 2862–2868.